

# Sol-Gel Processing of Inorganic Membranes for Natural Gas Purification

C. Jeffrey Brinker (cjbrink@sandia.gov; 505-272-7627)  
John Collins (jcolli@sandia.gov; 505-272-7623)  
Direct Fabrication Department, 1831  
Mail Stop 1349, Sandia National Laboratories  
P.O.Box 5800  
Albuquerque, NM 87185-5800

Chung-Yi Tsai (cytsai@unm.edu; 505-272-7634)  
Yungfeng Lu (yfnl@unm.edu; 505-272-7127)  
Advanced Materials Laboratories/University of New Mexico  
1001 University Blvd. SE Suite 100  
Albuquerque, NM 87106

DOE Award Number: 97MC28074

Research sponsored by the U.S. Department of Energy's Federal Energy Technology Center, under contract DE-AC04-94AL85000 with Sandia National Laboratories, P.O. Box 5800, Albuquerque, NM 87185-5800

## Executive Summary

This paper summarizes several sol-gel processes we have developed to prepare microporous silica membranes supported on commercial alumina supports for purification of natural gas. Based on single gas permeance measurements, our combined approaches have resulted in ideal separation factors (ratios of single gas permeances) in the range 30 to over 200 for CO<sub>2</sub>/CH<sub>4</sub> and in the range 15 to over 100 for N<sub>2</sub>/CH<sub>4</sub>. To our knowledge these preliminary results are the first to show feasibility of a membrane-based N<sub>2</sub>/CH<sub>4</sub> separation. Due to the higher intrinsic permeabilities of porous inorganic membranes compared to dense organic polymer membranes and our ability to prepare inorganic membranes as ultra-thin supported films (< 100 nm), the separation power of our membranes is estimated to be 1000 times greater than 25- $\mu$ m thick polyimide membranes for CO<sub>2</sub>/CH<sub>4</sub> separation. We propose surfactant-templating as a new approach to prepare inorganic membranes with potentially higher fluxes along with better control of pore size.

## I. Introduction

Due to their greater thermal and chemical stabilities and especially higher fluxes compared to organic polymer membranes, inorganic membranes are attractive for the purification of natural

gas. For practical gas separations, the membrane must combine high selectivity with high flux. Selectivity of porous membranes depends on the pore size and pore size distribution. When the pore size is reduced below the mean free path of a gas molecule, gas transport occurs by Knudsen diffusion, and the separation factor for a binary gas mixture depends on the inverse ratio of the respective molecular weights. For example, the Knudsen selectivity factor  $\alpha_K$  for a  $\text{CO}_2/\text{CH}_4$  mixture is 0.6. Therefore to remove carbon dioxide from methane it is necessary to further reduce the pore size and narrow the pore size distribution so that molecules are admitted and excluded on the basis of size, a mechanism referred to as molecular sieving. Flux of porous membranes is generally proportional to the product of porosity and pore size divided by the membrane thickness. Thus to combine high flux with high selectivity it is necessary to prepare extremely thin films with a large volume fraction of extremely small and narrowly distributed pores ( $r_p \sim$  molecule size) and no cracks or other imperfections that would serve as larger pores and diminish selectivity.

This report briefly reviews our progress on the development of ultra-thin (<100 nm), defect-free inorganic membranes with pore sizes in the range, 0.3 - 0.8 nm, for application in natural gas purification. First we describe our approach to avoid defect formation, which relies on the deposition of a thin external membrane layer that can shrink one-dimensionally during drying and heating without cracking. We then summarize three strategies that enable control of membrane pore size in the range appropriate for natural gas purification:

- Solvent-templating of the silica framework.
- The preparation of hybrid organic-inorganic membranes followed by extraction or pyrolysis of the organic constituents that serve as micropore templates.
- Surface derivatization of pre-formed membrane pore networks with well-defined molecular species.

We conclude the report with a description of a new template-based approach to prepare inorganic membranes with potentially higher fluxes more precise control of pore size.

## II. Results and Discussion

### II.1 Sol-Gel Processing of Defect-Free Membranes

In the sol-gel process,<sup>1</sup> *sols* colloidal dispersions of inorganic particles or polymers are prepared in alcohol water solutions by the hydrolysis and condensation of metal alkoxide precursors,  $\text{M}(\text{OR})_z$  where M is a metal, R is an alkyl group ( $\text{C}_n\text{H}_{2n+1}$ ), and z is the valence of the metal. Inorganic membranes are prepared by deposition of dilute sols on porous inorganic supports by dip-coating. In the dip-coating process,<sup>2</sup> the support is immersed in the sol and withdrawn vertically at a constant rate. During immersion, capillary suction causes flow of the sol into the pores of the support. During withdrawal, additional sol is metered onto the support surface. The depositing sol experiences evaporation leading to aggregation and gelation of the

entrained inorganic constituents. Beyond the gel point further evaporation causes the development of a tensile *capillary stress*  $P_c$  in the gel pore fluid. The magnitude of the stress is initially described by the Kelvin-Laplace equation:

$$P_c = 2\gamma_{LV} \cos(\theta)/r_p = -\ln(P/P_0) RT/V_m \quad (1)$$

where  $\gamma_{LV}$  is the surface tension,  $\theta$  is the wetting angle,  $r_p$  is the pore size,  $P/P_0$  is the relative pressures of the overlying vapor,  $R$  is the molar gas constant, and  $V_m$  the molar volume of the pore fluid/vapor.

The capillary stress causes film shrinkage which is manifested as a reduction in pore volume and pore size. Because shrinkage of the external membrane layer is completely accommodated by a reduction in film thickness, a biaxial tensile stress  $\sigma$  develops in the plane of the external membrane. (A three-dimensional stress develops within any gel formed within the pores of the underlying support). Scherer has shown that  $\sigma$  is approximately the capillary stress  $P_c$  developed in the liquid during drying. *Cantilever beam* bending experiments performed in our laboratory<sup>3</sup> have shown that the biaxial stress  $\sigma$  may be in excess of 200 Mpa (> 2 kbar), yet despite this high stress, cracking of the film is not observed if the film is below a *critical cracking thickness*  $h_c$  given by:<sup>4</sup>

$$h_c = (K_{Ic}/\sigma \Omega)^2 \quad (2)$$

where  $K_{Ic}$  is the critical stress intensity or "fracture toughness" and  $\Omega$  is a function that depends on the ratio of the elastic modulus of the film and substrate (for gel films  $\Omega \approx 1$ ). Since fracture toughness can be considered an intrinsic materials property, the drying stress and film thickness largely determine whether or not cracking will occur. In addition, it is the drying stress that establishes the extent of drying shrinkage and hence the pore volume and average pore size of the deposited membrane.

Based on Eq. 2, a strategy to prepare defect-free membranes is to grow the sol polymers to an average size greater than the pore size of the underlying support, allowing the formation of a discrete external membrane layer that experiences one-dimensional shrinkage. Through variation of the sol concentration or withdrawal rate to maintain the membrane film thickness below the critical thickness  $h_c$ , cracking is avoided. Figure 1<sup>5</sup> shows transmission electron microscopy images of cross-sections of membranes formed from polysiloxane sols prepared with polymer Guinier radii  $R_g$  smaller than, comparable to, or larger than the support pore size,  $r_s \approx 2$  nm. When the polymer size was less than  $r_s$ , silica deposition occurred only within the underlying support, but when the polymer size was comparable to or larger than  $r_s$ , a discrete external membrane layer was formed. By maintaining the film thickness  $h \ll h_c$  (estimated to be about 400 nm), not only is cracking avoided but membrane flux is enhanced. For membranes formed within the pores of the underlying support, finite element-based analyses<sup>6</sup> show that the drying stress is amplified (because shrinkage is constrained in three-dimensions), promoting defect formation.

## II.2 Control of Pore Size and Pore Size Distribution

To efficiently separate CO<sub>2</sub> (kinetic diameter = 0.33 nm) from CH<sub>4</sub> (kinetic diameter = 0.38 nm) or (harder still) N<sub>2</sub> (kinetic diameter = 0.364 nm) from methane, it is necessary to accurately control the average pore size between about 0.3 and 0.4 nm and achieve a narrow pore size distribution. To this end we have developed several synthesis and processing strategies that are briefly summarized in the following paragraphs.

**Solvent Templating** - As discussed above, the development of capillary stress in the pore fluid during drying causes shrinkage of the membrane. Shrinkage in turn causes a reduction in pore volume and average pore size. Thus one approach to create pores of molecular dimension needed for molecular sieving is to promote drying shrinkage. The conventional view of drying shrinkage is that it continues until capillary stress  $P_c$  is balanced by the network resistance<sup>7</sup> as expressed in the following equation where the left side represents the capillary stress and the right side, the network modulus:

$$P_c = -RT/V_m \ln (P/P_0) = K_0/m\beta C_n [(h_0/h)^m - 1], \quad (3)$$

and  $V_m$  is the molar volume of the pore liquid,  $K_0$  is the initial network bulk modulus at the gel point, the exponent  $m$  equals approximately 3,  $\beta$  and  $C_n$  are constants that depend on Poisson's ratio and the ratio of the network and skeletal moduli, and  $h_0$  is the film thickness at the gel point. Thus the final film thickness  $h$ , pore volume, and pore size - properties crucial to membrane performance - are in many cases established by the balance between the capillary tension and the network resistance (viscosity or modulus).

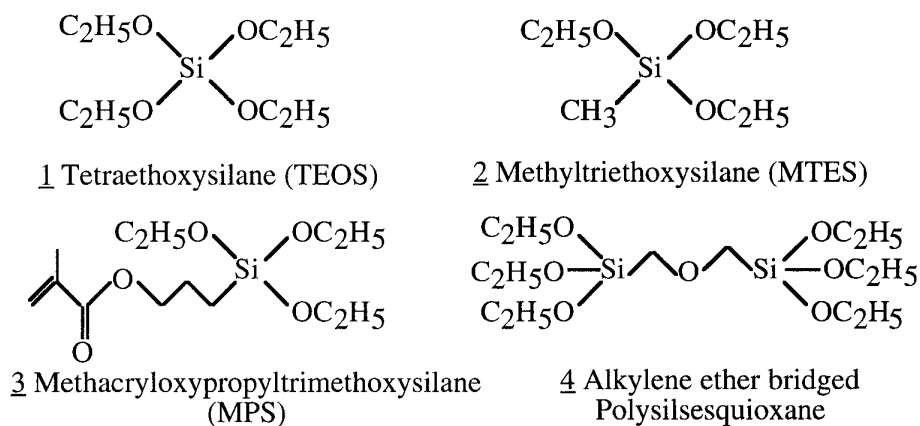
However if  $K_0$  is designed to be low through catalytic control of the extent of reaction and drying is carried out at low relative pressure  $P/P_0$ , the capillary stress may always exceed the network resistance, causing complete collapse of the developing gel network. In this situation, we may ask ourselves what controls the membrane pore size. Recently we have used *density functional theory* (DFT) to address this question.<sup>8</sup> DFT analyses indicate that in the limiting case where there is no network resistance, the final pore size is controlled by the relative pressure  $P/P_0$  of the pore fluid in the processing environment and the size of the pore fluid molecule  $\sigma_{PF}$ . Basically the pore size decreases with decreasing  $P/P_0$ , reaching a limiting value of about  $1.8 \sigma_{PF}$  at  $P/P_0 < 0.1$ . Therefore the pore size can be controlled by  $P/P_0$  and the choice of the pore fluid molecule, a mechanism we refer to as *solvent templating*.

We have recently demonstrated that by simply changing the solvent composition, it is possible to vary the *transport limiting* pore size in the approximate range  $0.3$  to  $0.8 \pm 0.05$  nm.<sup>9</sup> Using this approach with water as the solvent templating molecule we achieve membranes exhibiting unique thermal behaviors.<sup>9,10</sup> Figure 2 plots the single gas permeance of a series of molecules through a single layer silica membrane deposited at room temperature and partially sintered at 550 °C. Methane, the largest molecule of the series, does not permeate (detection limit  $10^{-7}$  cm<sup>3</sup>/cm<sup>2</sup>-sec-cm Hg). Nitrogen, the next largest molecule, permeates at high temperature, but, upon reduction of temperature, exhibits a sharp drop-off in permeance. With decreasing size of the permeating molecules, the permeance at high temperature shows a

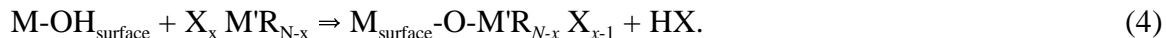
systematic increase and the drop-off temperature a systematic decrease. This type of behavior, heretofore unknown for microporous materials, results high selectivity factors (defined here as the ratio of the single gas permeances) for various pairs of gases in different temperature ranges (see Table 1). This suggests the possibility of thermally staged separation processes whereby a multicomponent process stream (e.g., natural gas) would be passed through a series of membranes maintained at progressively higher temperatures, allowing the successive removal of gases of increasing molecular size, i.e., He, CO<sub>2</sub>, and N<sub>2</sub>.

**"Fugitive" Organic Templates** - A natural limitation of the above approach is that the small pores needed for high selectivity result from the collapse of the developing network due to the imposed drying stress, so small pores are obtained at the expense of volume fraction porosity. A strategy designed to overcome this limitation (to membrane flux) is to prepare dense, hybrid organic-inorganic membranes and create porosity by the removal of the organic constituents.<sup>11,12</sup> When organic ligands are molecularly dispersed within an inorganic framework, their removal should create pores that mimic the size and shape of the fugitive ligand (see Figure 3), so pore size is controlled by the organic *template* size. Additionally, through variation of the volume fraction of organic ligands, it is possible to control membrane porosity and hence flux.

Our approach in this area has been to synthesize co-polymers from tetra-functional alkoxides, e.g. tetraethoxysilane (TEOS) **1**, and organo-substituted alkoxides, e.g., methyltriethoxysilane (MTES) **2**, methacryloxypropylsilane (MPS) **3**, or 4,4'-bis(triethoxysilyl)biphenyl incorporating non-hydrolyzable organic "template" ligands in either pendant or bridging positions. We find that for synthesis and processing conditions under which phase separation is suppressed, the pores created by oxidative ligand pyrolysis scale in size with the size of the template ligands. Using this approach combined with surface derivatization (see discussion below) we have prepared a variety of membranes with ideal CO<sub>2</sub>/CH<sub>4</sub> selectivities as high as seventy with CO<sub>2</sub> fluxes in the range 2-5 x 10<sup>-4</sup> cm<sup>3</sup>/cm<sup>2</sup> s cm Hg).<sup>11,13</sup>



**Surface Derivatization** - A strategy that can be combined with either of the above approaches is to modify or "derivatize" the pore surface through liquid or vapor phase reactions of the general type:<sup>14</sup>



where M and M' are metals, N is the coordination number of M', X is typically a halide or alkoxide ligand, and R is an organic ligand. For example, the silanol ( $\equiv\text{Si-OH}$ ) surface inherent to the silica membranes can be titrated with well-defined metal alkoxide species (see Figure 4) to reduce the pore size in an angstrom-by-angstrom manner. When  $\text{M} \neq \text{Si}$ , this process also alters the surface chemistry. Through derivatization of a larger pore size silica membrane with a monomeric titanium alkoxide, we obtain membrane performance comparable to that shown in Figure 1.<sup>10</sup> In addition this derivatization step both increases the chemical stability of the membrane and affords a means to deposit ion-exchangeable amorphous titanates or photocatalytically active nanocrystalline titanates (anatase) on the membrane surface for applications in catalytic membrane reactors.

The surface chemistry can also be altered by the processing gas used for partial sintering and pyrolysis of the organic constituents. For example, when the organic template ligands described above are pyrolyzed under reducing conditions (flowing argon) the membrane is rendered hydrophobic, increasing the membrane stability in the presence of water.<sup>13</sup>

Overall, the combined approaches summarized above result in a series of membranes with combined  $\text{CO}_2/\text{CH}_4$  selectivities and  $\text{CO}_2$  permeabilities exceeding those of organic polymer membranes. This comparison is made in Figure 5.

### II.3 Surfactant-Templating of Inorganic Membranes

Recently Kresge and et al.<sup>15</sup> reported on a family of mesoporous silicas formed by *surfactant-templating*. Surfactant-templated silicas (STS) are high surface area amorphous solids (up to  $1400 \text{ m}^2/\text{g}$ ) characterized by monosized, often cylindrical pores, ranging normally from 20-100 Å in diameter, organized into periodic arrays that often mimic the liquid crystalline (LC) phases exhibited by surfactant-water systems. STS synthesis procedures typically require four reagents: water, a soluble inorganic precursor, catalyst and surfactant (an amphiphilic molecule composed of a hydrophilic head group and hydrophobic tail). STS form (as precipitates) in seconds to days at temperatures ranging from  $180^\circ\text{C}$  to as low as  $-14^\circ\text{C}$ , depending on the inorganic precursor. Pure silica STS exhibit three structure types: hexagonal, a 1-D system of hexagonally ordered cylindrical pores; cubic, a 3-D, bicontinuous system of pores; and lamellar, a 2-D system of silica sheets interleaved by surfactant bilayers (see Figure 6).<sup>16</sup>

From the standpoint of membrane-based separations, STS are of interest because of their similarities to zeolites, *viz.* high porosity, low pore tortuosity, and precise control of pore size. However to date, they have been prepared mainly as powders rather than films and their pore sizes are too large for molecular sieving. Recent work in our group<sup>17</sup> has shown that STS can be prepared by continuous dip-coating operations amenable to membrane formation. Preliminary single gas permeance experiments suggest that STS membranes deposited on  $\gamma\text{-Al}_2\text{O}_3$  supports are defect-free, and x-ray diffraction (XRD) and TEM experiments have shown that we can prepare hexagonal, cubic, or lamellar films depending on the initial surfactant concentration.

Figure 7a shows a cross-sectional TEM micrograph of a cubic STS film prepared on single crystal  $\langle 100 \rangle$  silicon, using  $C_{16}$  trimethylammonium bromide ( $C_{16}$  TAB) as surfactant. The film was pyrolyzed at  $400\text{ }^{\circ}\text{C}$  to remove the surfactant and further condense the silica framework. Despite the fact that considerable shrinkage occurs upon pyrolysis ( $\sim 30\text{ vol } \%$ ), we see a uniform film texture consistent with a unimodal pore size distribution. TEM, XRD, and gas sorption analyses indicate that the pore radius is about  $1.0\text{ nm}$ , with about a  $1\text{-nm}$  wall thickness. Ellipsometry indicates a porosity of about  $50\%$ . Figure 7b shows a higher magnification of a cubic film oriented along the  $\langle 210 \rangle$  zone axis. We observe a very well ordered pore structure.

At least two possibilities exist for reducing the pore size of STS to the  $0.3\text{-}0.5\text{-nm}$  range needed for natural gas purification: 1) Experiments on bulk STS mesophases have shown that the pore size decreases monotonically with the size of the hydrophobic tail of the surfactant template.<sup>16</sup> We anticipate that ordered STS membranes can be prepared with  $c_8$ -surfactants which should reduce the pore size to  $r_p \approx 0.5\text{ nm}$ . 2) The interior surfaces of the pores are covered with silanol groups ( $\equiv \text{Si-OH}$ ), enabling surface derivatization with well-defined metal alkoxides (see Fig.4) or organosilanes (e.g.  $\text{ClSi}(\text{CH}_3)_3$ ). Used individually or in combination, approaches 1 and 2 should enable precise control of pore size. In addition, approach 2 can be used to render the pore surface hydrophobic or to otherwise alter the pore surface chemistry.

### III. Conclusions

Our project to date has demonstrated the feasibility of using microporous inorganic membranes to purify natural gas. Three approaches have been developed to control the membrane pore size in the range  $0.3\text{-}0.5\text{-nm}$  range necessary to selectively remove  $\text{CO}_2$  or  $\text{N}_2$  from methane: 1) solvent- templating of the silica framework, 2) pyrolysis of organic ligands from dense hybrid organic-inorganic membranes, and 3) surface derivatization of pore surfaces with metal alkoxides. The intrinsic higher permeability of microporous inorganic membranes compared to dense organic polymer membranes combined with our ability to prepare inorganic membranes as ultra-thin supported films enables us to achieve higher  $\text{CO}_2$  flux with ideal  $\text{CO}_2/\text{CH}_4$  selectivities comparable to or greater than organic polymer membranes. We have identified a promising new surfactant-templating approach to prepare inorganic membranes. This approach combines the high porosity and control of pore size inherent to zeolite membranes with the ease of processing of organic polymer membranes.

The future goals of this project include:

- Testing of membranes using dual/multiple gas permeance measurements.
- Preparation of hydrophobic, microporous membranes to enhance long term stability.
- Modeling of gas transport in microporous inorganic membranes.
- Development of new candidate membrane materials with improved selectivity and flux.

- Adaptation of our membrane technology to low cost, high surface area hollow fiber supports.
- Definition of processing windows to routine manufacture of inorganic membranes and technology transfer to the commercial sector.

## IV. Acknowledgments

Authors would like to acknowledge co-sponsorship of this program by the Federal Energy Technology Center, the Gas Research Institute, the Electric Power Research Institute, and the National Science Foundation Division of Chemical and Transport Systems. We would also like to acknowledge the help and encouragement of Harold Shoemaker, Venkat K. Venkataraman, and Tony Zammerilli who have managed the project since its inception in July, 1991.

## V. References

1. C.J. Brinker and G.W. Scherer, Sol-Gel Science-The Physics and Chemistry of Sol-Gel Processing (Academic Press, San Diego, 1990).
2. C.J. Brinker, G.C. Frye, A.J. Hurd, and C.S. Ashley, *Thin Solid Films* **201** (1991) 97-108.
3. Mengcheng Lu, *unpublished results*.
4. M.D. Thouless, *Acta Metall.* **36** (1988) 3131-3135.
5. C.J. Brinker, N.K. Raman, M.N. Logan, R. Sehgal, R.A. Assink, D.-W. Hua and T.L. Ward, *J. Sol-Gel Sci. and Tech.* **4** (1995) 117-133.
6. R.A. Cairncross, P.R. Schunk, K.S. Chen, S.S. Prakash, J. Samuel, A.J. Hurd, and C.J. Brinker, *Sandia National Laboratory Report, SAND96-2149* September 1996.
7. G.W. Scherer, *J. Non-Cryst. Solids* **155** (1993) 1.
8. J. Samuel, C.J. Brinker, L.J. Douglas-Frink, and F. van Swol, *Phys. Rev. Lett.*, submitted.
9. C.J. Brinker, S. Wallace, N.K. Raman, R. Sehgal, J. Samuel, and S.M. Contakes, "Sol-gel processing of amorphous nanoporous silicas: thin film and bulk", in Access in Nanoporous Materials, edited by T.J. Pinnavaia and M.F. Thorpe (Plenum Press, New York, 1995) pp 123-139.
10. R. Sehgal and C.J. Brinker, "Supported Inorganic Membranes", *U.S. Patent Application Serial No. 08/551,956* (November 2, 1995).

11. N.K. Raman and C.J. Brinker, *J. Membrane Sci.* **105** (1995) 273-279.
12. G.Z. Cao, Y.F. Lu, L. Delattre, C.J. Brinker, and G.P. Lopez, *Adv. Mater.*, **8** (1996) 588-591.
13. N.K. Raman and C.J. Brinker, "Organic Template Approach to Molecular Sieving Membranes", *U.S. Patent Application Serial No. 08/702, 745* (August 23, 1996).
14. C.J. Brinker, R. Sehgal, N.K. Raman, S.S. Prakash, and L. Delattre, *Mat. Res. Soc. Symp. Proc.*, **368** (1995) 329-343.
15. C.T. Kresge CT, M.E. Leonowicz, W.J. Roth, J.C. Vartuli, J.S., *Nature* **359** (1992) 710-712.
16. N.K. Raman, M.T. and C.J. Brinker, *Chem. Mater* **8** (1996) 1682-1701.
17. R. Ganguli, et al. *Nature*, submitted.

(a)  $t/t_{\text{gel}} = 0.05$



(b)  $t/t_{\text{gel}} = 0.24$



(c)  $t/t_{\text{gel}} = 0.83$

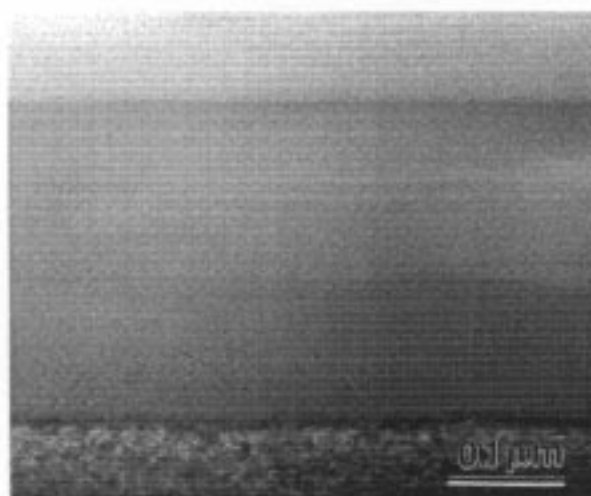


**Figure 1.** Cross-sectional TEM micrographs of microporous silica membranes deposited on  $\gamma$ - $\text{Al}_2\text{O}_3$  supports after various sol aging times  $t/t_{\text{gel}}$  used to control the precursor polysiloxane Guinier radius  $R_g$  measured by small angle x-ray scattering. Energy dispersive spectroscopy analysis indicated that for  $t/t_{\text{gel}} = 0.05$ , silica deposition occurred exclusively within the pores of the support.

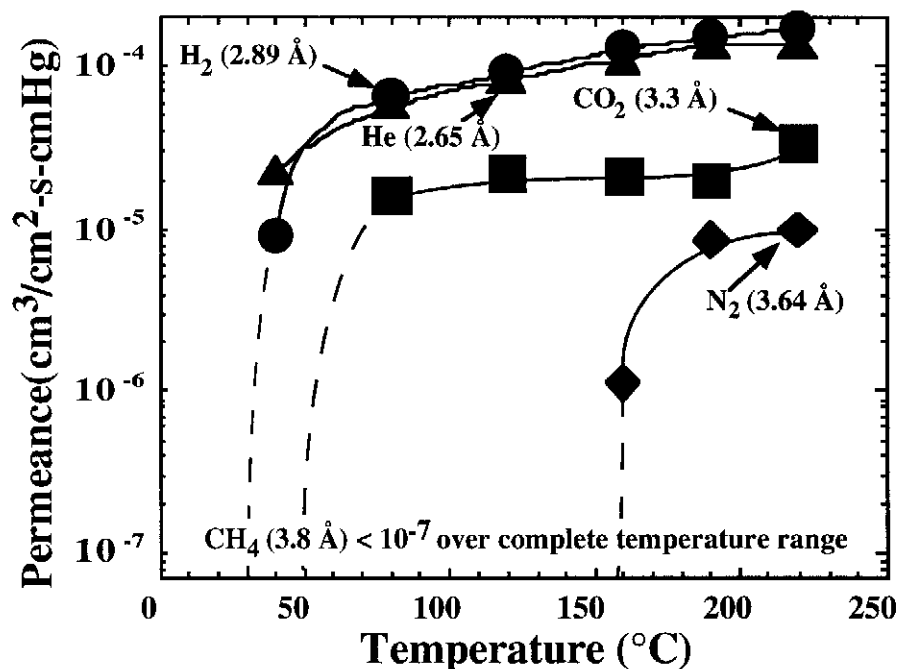


**Figure 2.** Single gas permeance of a series of five gases versus temperature for a microporous silica membrane. Dotted line corresponds to the predicted behavior of O<sub>2</sub>.

T (°C)	He Perm	$\alpha_{\text{He}/\text{H}_2}$	$\alpha_{\text{He}/\text{N}_2}$	$\alpha_{\text{He}/\text{CO}_2}$	$\alpha_{\text{He}/\text{CH}_4}$	$\alpha_{\text{CO}_2/\text{CH}_4}$	$\alpha_{\text{N}_2/\text{CH}_4}$
220	1.36e-04	0.80	14.06	4.00	>2000	>400	>100
190	1.35e-04	0.89	16.19	6.61	>2000	>300	>90
160	1.11e-04	0.87	100.1	5.36	>1500	>300	>15
120	8.20e-05	0.90	>900	3.71	>900	>200	*
80	5.62e-05	0.87	>800	3.44	>800	>200	*
40	2.25e-05	2.5	>300	>200	>500	*	*

\*: indicates that both the gases were below the resolution of the system.

Table 1. Ideal selectivities (ratio of single gas permeances) versus temperature based on the data shown in Figure 2.

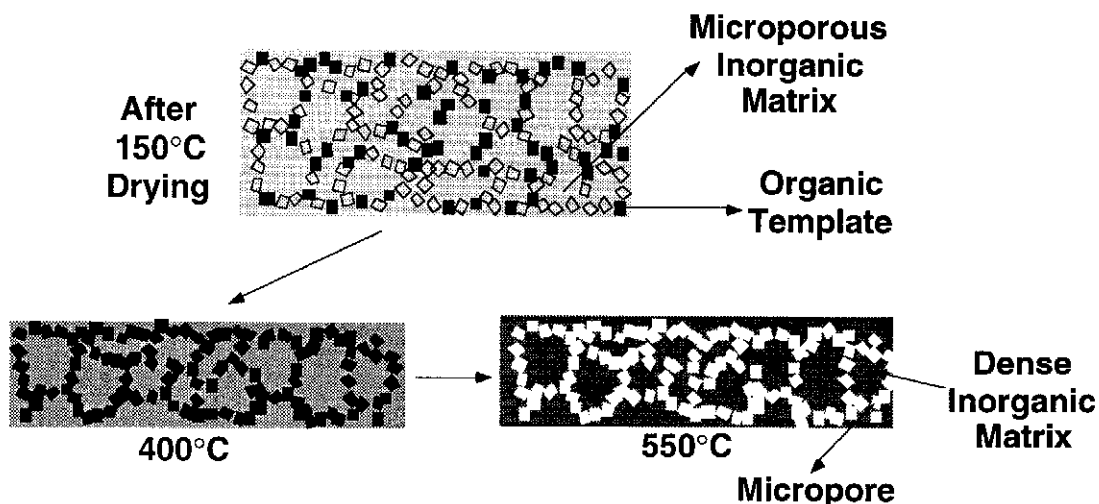


**Figure 3.** Schematic illustration of the organic template approach. Incorporation of the organic templates in a dense matrix followed by their removal creates a microporous network that mimics the original dispersion of the occluded organic ligands.

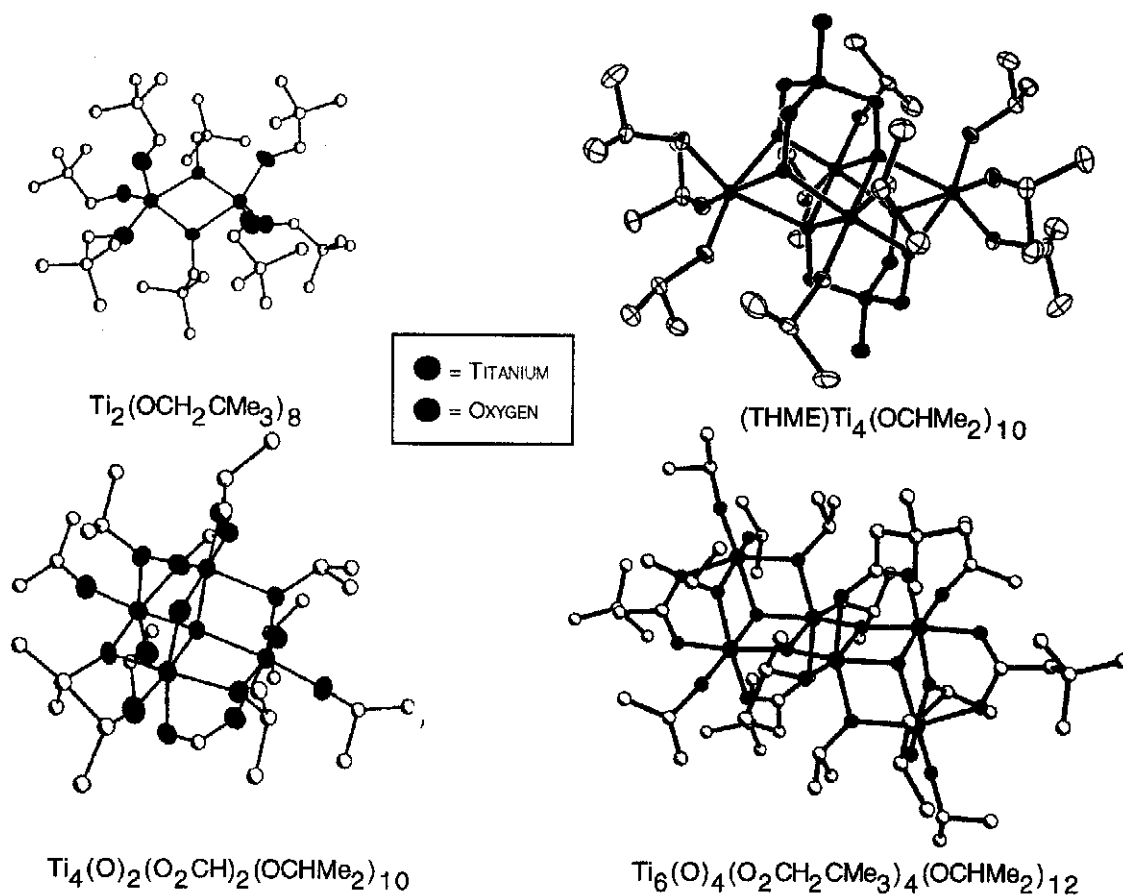


**Figure 4.** Crystal structures of several titanium alkoxides  $[\text{Ti}(\text{OR})_4]_n$  and titanium oxoalkoxides that could be used to derivatize the pore surfaces of microporous inorganic membranes in order to precisely reduce the pore size.

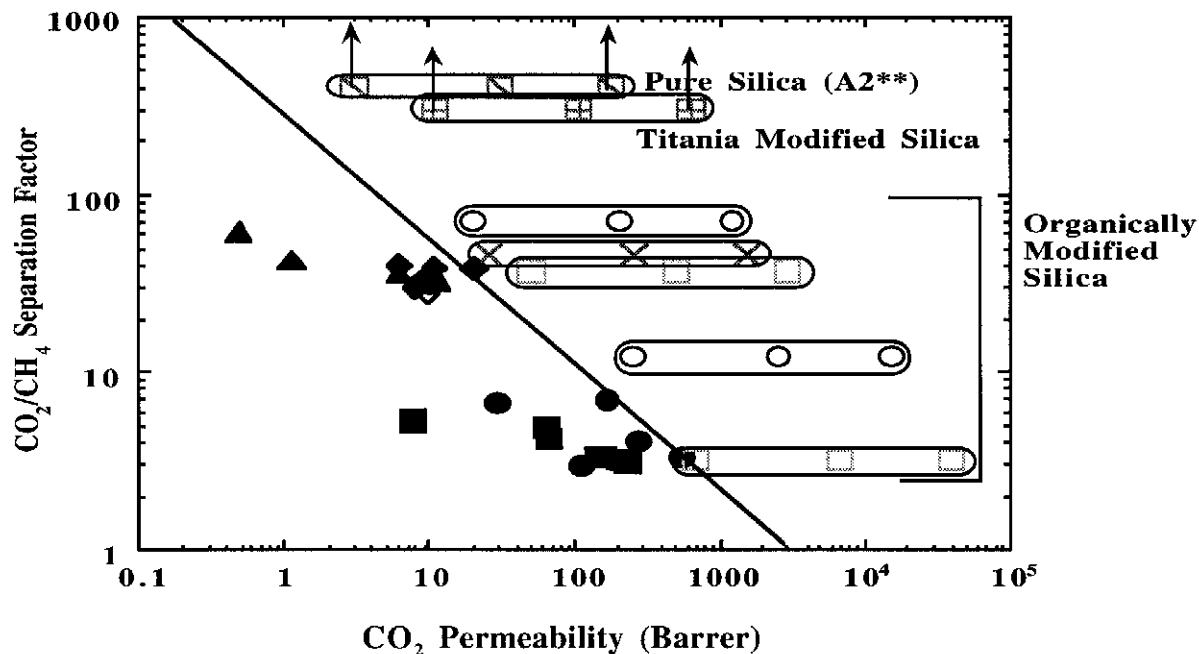


**Figure 5.** Log-log plot of CO<sub>2</sub>/CH<sub>4</sub> separation factors versus CO<sub>2</sub> permeabilities for the best organic membranes reported in the literature (cf Robeson, J. of Membrane Sci. 62 (1991) 165-185) and microporous silica and derivatized silica membranes described above.

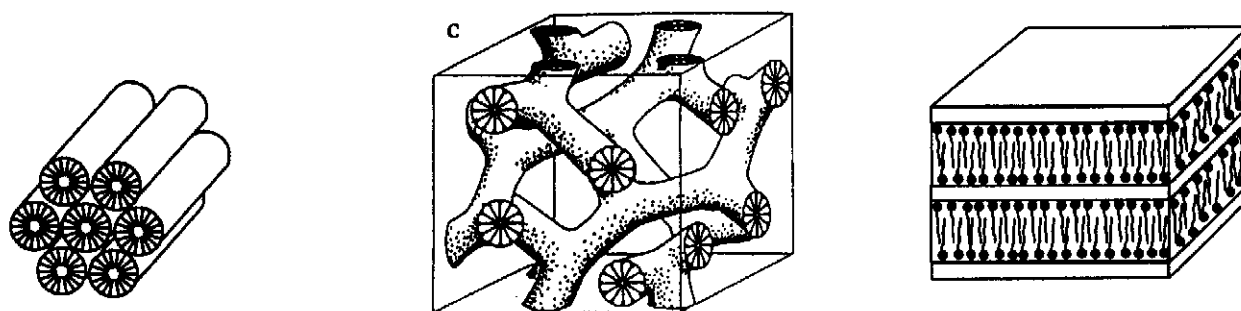


**Figure 6.** Schematic representation of the three observed liquid-crystalline phases of surfactant-templated silicas (STS) (left-hexagonal; center-cubic, bicontinuous, right-lamellar). In each case the supra-molecular surfactant assembly co-assembles with soluble silica adjacent to the hydrophilic surfactant head groups. Upon pyrolysis or extraction of the surfactants, a silica skeleton remains with precise pore size, shape, and orientation.

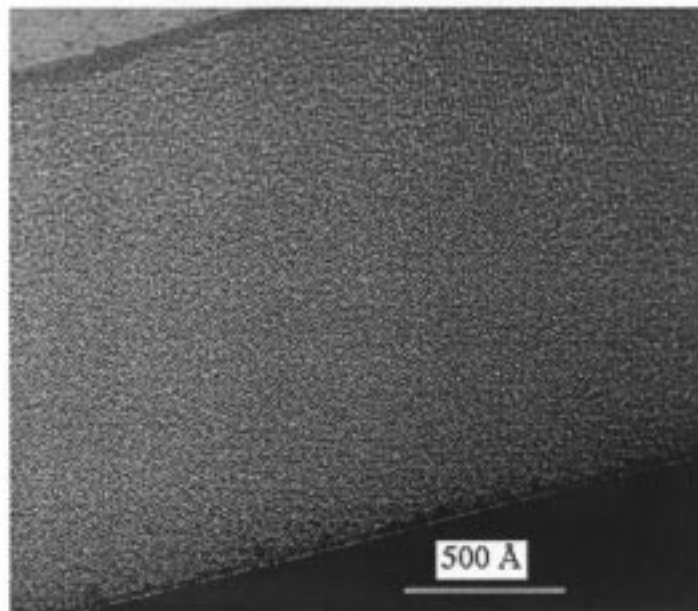


**Fig. 7a.** Cross-sectional TEM micrograph of a cubic surfactant-templated silica film deposited on  $\langle 100 \rangle$  single crystal silicon and pyrolyzed at 400°C.

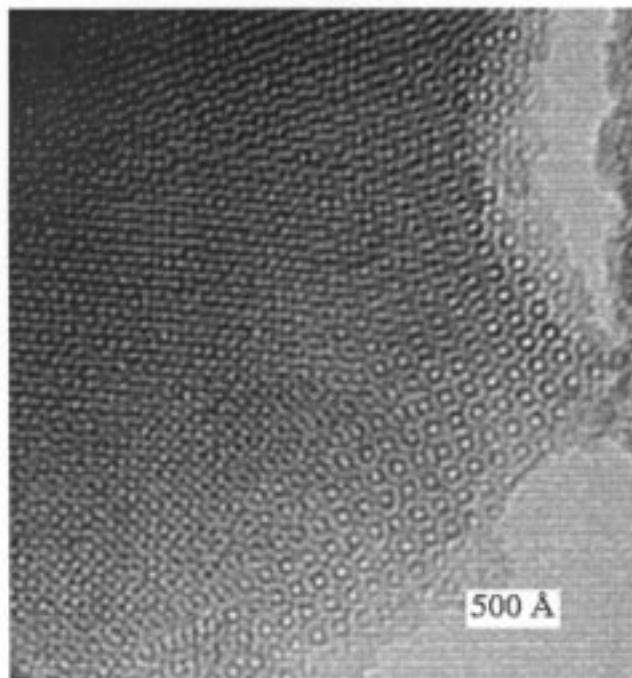


**Fig. 7b.** Thin flake of cubic surfactant-templated silica film prepared as in Figure 7a suspended on a holey carbon grid.